British Journal of Environmental Sciences

Vol.7, No.2, pp. 31-58, May 2019

Published by European Centre for Research Training and Development UK (www.eajournals.org)

MAPPING OF LAND COVER AND ESTIMATION OF THEIR EMISSIVITY VALUES FOR GAS FLARING SITES IN THE NIGER DELTA

Barnabas Morakinyo[1, 2,3,4], Samantha Lavender[2,3], Jill Schwarz[2] and Victor Abbott[2]

(1) Department of Surveying & Geoinformatics, Faculty of Environmental Sciences, Baze University, Abuja, Nigeria;

(2) School of Marine Science & Engineering, University of Plymouth, Plymouth, UK

(3) Pixalytics Ltd, 1 Davy Rd, Tamar Science Park, Plymouth, Devon, PL6 8BX, UK

(4) ARGANS Ltd, 1 Davy Rd, Tamar Science Park, Plymouth, Devon, PL6 8BX, UK

ABSTRACT: *This study examines the changes in land cover (LC) types at 6 gas flaring sites in Rivers State, Niger Delta region of Nigeria; and to estimate their emissivity (Ɛ) values. 15 Landsat scenes (3 Landsat 5 Thematic Mapper (TM) and 12 Landsat 7 Enhanced Thematic Mapper Plus (ETM+)) from 17 January 1986 to 08 March 2013 with < 30 % cloud contamination were used. All the sites are located within a single Landsat scene (Path 188, Row 057). Radiometric calibration of the multispectral bands of the data, and atmospheric correction for multispectral bands using dark object subtraction (DOS) method was carried out. The first unsupervised cluster analysis of the atmospherically corrected reflectance (bands 1-4) using the K-mean function of the MATLAB tool was carried out. The results obtained give 3 classes of LC type and cloud as the 4th class. The second cluster analysis was performed with the cloud-masked reflectance (bands 1-4) to give vegetation, soil, built up area and water LC types for all flaring sites. This was confirmed through the fieldwork observation for ground validation of Landsat 5 TM and Landsat 7 ETM+ in the Niger Delta that LC types obtained from satellite data are the same with those observed during the fieldwork. The method used to estimate Ɛ value for LC types at these sites is based on the Ɛ of 4 LC types present at each site. The changes in LC differ throughout the period for the 6 sites due to different human activities within each site. The Ɛ values estimated for the 4 LC types for the sites are not stable but changing from 1986 to 2013 due to changes in LC types. The results of LC classification show that K-mean method can distinguish up to 4 LC types very well in the Niger Delta.*

KEYWORDS: Mapping, land cover, emissivity, estimation, gas flaring, Niger Delta.

THEORETICAL BACKGROUND

Remote sensing (RS) of land cover (LC) classification is a vital research subject world-wide (Morakinyo, 2015). RS technology provides the basis and data for land use/land cover (LULC) with dynamic monitoring and quantitative analysis (Yue et al., 2018). LC is considered to be the biophysical state of the Earth's surface and its upper subsurface while land use is the utilization, human inputs and management levels on the Earth's surface, driven by production and consumption dynamics that are closely tied to social, political and economic activities, leading to LC modification (Schulze, 2000). LC has a unique signature on the topography and soil distribution that gives rise to natural resource changes (Hu et al., 2005). Monitoring of LULC through Earth Observation Satellite data has the advantages of fast, real-time, visible characteristics etc., especially over a large area (Yuechen et al., 2012). Land surface

ISSN 2054-6351 (print), ISSN 2054-636X (online)

characteristics are primarily represented by LULC (Boori et al., 2015; Antonarakis et al., 2008). Roberts et al. (1998) described LC change as the most significant regional anthropogenic disturbance to the environment. LC changes are products of prevailing interacting natural and anthropogenic processes by human activities (Ademiluyi et al., 2008; Lambin, 2003) due to population increase, the spread of settlement and increasing use of land resources for economic development such as oil exploration and exploitation, and agriculture (Ouedraogo, 2010; Braimoh and Vlek, 2004; Lambin, 2003). LC change and land degradation are driven by the same set of imminent and underlying factor elements central to environmental processes, change and management through their influence on biodiversity, heat and moisture budgets, trace gas emissions, carbon cycling, livelihoods and a wide range of socio-economic and ecological processes (Fasona and Omojola, 2005; Verburg et al., 2002; Desanker et al., 1997).

There has been a global increasing awareness and studies on LC change analysis more than 6 decades ago. The significance of such studies to global climate change, and sustainable development plan of nations has also been internationally acknowledged (Yue et al., 2018; Hua et al., 2015). Some research shows that more than 100 years ago, CO_2 emission to the atmosphere under the influence of LULC is equivalent to the industrial era of fossil fuel emissions to the atmosphere, which accounts for 35 % of the total CO_2 emission from human activities into the atmosphere (Hua et al., 2015; Huajun, 2009). LULC change reflect the pattern of interactions between human activities and the ecological environment (Pareta, 2014); and that LULC one of the main driving forces of global environmental change (Hegazy and Kaloop, 2015). LULC plays an important role in space soil and water conservation and has a direct impact on the global water-land-carbon cycle and balance of energy and a number of regional ecological balance (Yue et al., 2018). The timely update of LULC classification is of great importance to global change and environmental monitoring (Yuechen et al., 2012) and helps to simulate changes (Tomar et al., 2017). LULC is a central component in current strategies in managing natural resources and monitoring environmental changes (Maaharjan, 2018). The LU change has been shifted from LU planning and management to LU change impact and driving factors (Yue et al., 2018). Current LULC databases consist of Globeland30 (Yue et al., 2018); National Land Cover Data (NLCD) (Yuechen et al., 2012) etc.

Due to the seriousness of LULC changes on environment, a lot of impact studies have been done by researchers to improve understanding of connections between LU and the environment (Reid et al., 2005). Carleer and Wolff (2006) combined spectral information from IKONOS, Quick Bird, and OrbView-3 with visual interpretation to study LC classification. They stated that visual impression is a good means to guide the feature choice for LC classification; however it prevents the choice of a specific feature in the main feature types that can contain numerous features. They concluded that contrast between the vegetation and the non-vegetation is lower. Patrono (1996) observed that small discrepancies can be detected when combining the Landsat data with Satellite Pour l'Observation de la Terre (SPOT) data. However, he suggested that such discrepancies highlight the benefit of the combined use of different sensors in LULC studies especially in terms of resolution. Yuechen et al. (2012) used QuickBird data, SPOT data, Landsat 5 Thematic Mapper (TM) data, aerial images and vegetation data to distinguish and analyse 3 classes of LC.

ISSN 2054-6351 (print), ISSN 2054-636X (online)

In addition, Gong et al. (2006) combined airborne remote sensing data and ground survey data for LULC studies and analysis. Aixia et al. (2006) used MODerate Resolution Imaging Spectroradiometer (MODIS) data, Landsat 7 Enhanced Thematic Mapper Plus (ETM+) data, and Land Surface Temperature (LST) and Normalized Difference Vegetation Index (NDVI) time series datasets for LC classification. Advanced Spaceborne Thermal Emission and Reflection Radiometer (ASTER) data of 2003 with a spatial resolution of 15 m was employed by Rahman et al. (2012) for analysis of LC change. Maaharjan (2018) employed Landsat 8 Operational Land Imager (OLI) and Thermal Infrared Sensor (TIRS) C1 Level-1 and Landsat 5 TM C1 level -1 for LC classification. Fonteh et al. (2016) investigated, compared and integrated the use of Sentinel-1 C band Synthetic Aperture Radar (SAR) and Landsat 7 ETM+ for extracting LULC information in the coastal area. They stated that Sentinel-1 only, yielded a lower overall classification accuracy of 67.65 % when compared to all Landsat 7 ETM+ bands of 88.7 %. The integrated Sentinel-1 and Landsat 7 ETM+ showed no significant differences in overall accuracy assessment of 88.71 % and 88.59 % respectively. The 3 best spectral bands (5, 6, 7) of Landsat imagery yielded the highest overall accuracy assessment of 91.96 %. These results demonstrate a lower potential of Sentinel-1 for LC in the humid environment when compared with cloud free Landsat images (Fonteh et al., 2016). Textural variables including mean, correlation, contrast and entropy were derived from the Sentinel-1 C band (Fonteh et al., 2016). Yeboah et al. (2017) and Pareta (2014) acquired Landsat 5 TM, Landsat ETM+, field data and Google Earth imagery (Tomar et al., 2017) for LULC studies and change detection; Braimoh and Vlek (2004) undertook LULC in the Volta Basin part of Ghana; and Forkuo and Adubofour (2012) quantified the forest cover change patterns in the Owabi area in the Ashanti Region of Ghana and demonstrated the potential of multi-temporal satellite data to map and analyse changes in LC in spatio-temporal framework.

In Nigeria, few researchers on LULC studies includes Nnaji et al. (2016) who carried out spatio temporal analysis of LULC changes in Owerri Municipal and its environs, Imo State, using Landsat 7 ETM+ of 1991, 2001 and 2014. They distinguished 6 classes of LC (built-up area, open space, forest, farmland, vegetation and water bodies). They concluded that the rate of change shows that built up area was on continuous increase and open space was on a continuous decrease throughout the study period. Awoniran et al., (2013) investigated LULC change of the lower Ogun River Basin between 1984 and 2012 using a Landsat 5 TM data (1984), Landsat 7 ETM+ data (2000), and a Google Earth image of 2012. The result shows that between 1984 and 2000, 80.08 % of the LC in the study area has been converted to other LU while only 19.92 % remained unchanged. Also, Tokula and Ejaro (2012) used Landsat 7 ETM+ (1987); Landsat 5 TM (2001) and (2011) for the classification of agriculture land, bare soil, vegetation, and built up LC types. They concluded that most of agriculture land and vegetation were converted to built up areas.

Furthermore, Agoha (2009), analysed rural-urban LU change in Umuahia, Abia State, between 1991 and 2007 and observed that builtup area increased over the study period while agricultural land and vegetation depreciated significantly. Similarly, Ejaro, (2008) undertook analysis of LULC change in the Federal Capital Territory (FCT), Abuja, using Landsat data from 1973 to 2006. The results show that the proportion of area covered by built up land and bare surface was on increase while there is an alarming decline in vegetation and agricultural land. He stated that the geographical location, political and socio-economic activities and importance of the

ISSN 2054-6351 (print), ISSN 2054-636X (online)

FCT, which cause the rapid growth of human population and expansion, are the major reasons that have greatly influenced the changes in LULC in the FCT, Abuja especially reducing vegetation cover. Olowolafe et al. (2010) and Idowu and Muazu (2010) studied LULC and change detection; they found that agricultural land increased by 2.18 km^2 (28.17 %). They attributed the increase in agricultural land to the adoption of new agricultural practices which made some un-usable land before 2008 usable due to provision of agricultural incentives such as fertilizers supplies and irrigation by Katsina State Government.

However, there is still a low level of recognition and research attention on LC types studies in Nigeria (Okude, 2006). Only a small number of studies on mapping of LULC have been undertaken in Nigeria despite the increasing worldwide (Ademiluyi et al, 2008). The diversity is decreasing and the need to balance human well-being and environmental sustainability involves adjusting the way the ecosystem goods and services produced by the land are used**.** According to Ringrose et al. (1997), LULC change in Africa is currently accelerating and causing widespread environmental problems and thus needs to be mapped. This is important because the changing patterns of LULC reflect changing economic and social conditions. Monitoring such changes is important for coordinated actions at the national and international levels (Bernard and Wilkinson, 1997). At present, some problems in LULC change research can be grouped as: (a) Insufficient data from other land surveying methods except remote sensing data which is influenced by weather, precision of equipment, etc. (b) Most of the LULC models are greatly affected by the regional environmental factors, causing the function of the established models not to be well represented globally due to the limitation of data quality. (c) There is no unified theoretical system for reference, so the methods and models used by researchers have obvious regional limitations (Yue et al., 2018).

Emissivity (Ɛ) is the ratio of energy emitted from a natural material to that from an ideal blackbody at the same temperature (Mallick et al., 2012). An accurate value of surface Ɛ is desired in land surface models for better simulations of surface energy budgets from which skin temperature is calculated (Jin et al., 1997). The Ɛ of natural land surface is determined by soil structure, soil composition, organic matter, moisture content, and vegetation cover characteristics (Van de Griend and Owe, 1993). The Ɛ value always lies between 0 and 1 (Jin and Liang, 2006). The knowledge of surface Ɛ is important for estimating the land surface temperature (LST). It can reduce the error in estimating the surface temperature from thermal satellite data. Remotely sensing a surface Ɛ is very challenging because of the high heterogeneity of land surfaces and the difficulties in removing atmospheric effects (Liang, 2004; Liang, 2001; Wan and Li, 1997). Current Ɛ databases consist of MODIS, ASTER and Landsat products (Mallick et al., 2012).

Researchers have worked on Ɛ, for example Pu et al. (2006) used a constant value of Ɛ= 1 for all materials, although the authors stated that it is not a wise decision. Peng et al. (2008) and Xu et al. (2008) retrieved spectral Ɛ over urban areas in a pixel-by-pixel basis. Furthermore, many studies have been carried out in order to retrieve land surface Ɛ, such as temperature-independent spectral indices (TISI) methods (Zhu, 2006; Becker and Li, 1995; Li and Becker, 1993). This algorithm combines middle wave infrared data (MWIR: 3.4-5.2 µm) with thermal infrared data (TIR: 8-14 µm) to estimate Ɛ. Gillespie et al. (1998) developed this method for ASTER data and estimated Ɛ with high accuracy. However, the accuracy of this algorithm

ISSN 2054-6351 (print), ISSN 2054-636X (online)

depends on some assumptions and ties to the atmospheric correction. NDVI methods proposed by Caselles and Sobrino (1989) and developed by van de Griend and Owe (1993) supplied a technique to calculate Ɛ, and its successful performance in natural surface. But this method was based on the assumption that the land surface is mainly made up of vegetations and soil, which is not in agreement with land surface. Jimenez-Munoz et al. (2006) used NDVI based Ɛ method to obtain surface Ɛs over agricultural areas from ASTER data, and found that band 13 gave most accurate Ɛ measurement. Wan and Dozier (1996) utilized a classification-based Ɛ method and applied results to split window method, which performed satisfactorily. Snyder et al. (1998) also used this method to retrieve global Ɛ without considering the complicated urban surface heterogeneous.

Emissivity has strong seasonality and LULC dependence (Mallick et al., 2012). Specifically, Ɛ depends on surface cover type, soil moisture content, soil organic composition, vegetation density, and structure (Mallick et al., 2012; Jin and Liang, 2006). For example, the broad band Ɛ is usually around 0.96-0.98 for densely vegetated areas [(leaf area index) LAI > 2], but can be lower than 0.90 for bare soils (e.g., desert) (Jin and Liang, 2006). The accuracy of LC classification determines the value of the map obtained and that of the Ɛ value for each LC type (Morakinyo, 2015). However, the assessment of classification accuracy is not a simple task (Foody, 2002).Therefore, this call for an urgent action to understand the changing pattern of LC cover at the flaring sites in order to assess the extent of damage caused by the human activities and flaring.

In summary, limited research into LULC in the Niger Delta has been published to date, and no studies applied K-mean function of MATLAB tool methodology for the classification of LC types over time in the Niger Delta. In addition, there have been no publications on the Ɛ values for LC at the flaring sites in the Niger Delta. Hence, the 3 research questions for this paper are: (1). How accurately can we distinguish different LC types at flaring sites using K-mean MATLAB tool? (2). How accurately can Ɛ values be estimated from the LC map? (3). What is the % of LC change as a result of impacts of human activities on land over a period of time? Based on these research questions, the aim of this paper is to map LC types at gas flaring sites in the Niger Delta from 1986 to 2013 using K-mean MATLAB tool; and estimates the Ɛ values for these LC types. In order to answer the above research questions, specific objectives have been set: (1). Mapping and classification of LC types at the flaring sites using K-mean MATLAB tool; (2). Estimation of Ɛ values from LC types; and (3). Evaluation of the % of LC change caused by the impacts of human activities within the site from 1986 to 2013.

Study area

This study focuses on 6 gas flaring sites located in Rivers State of the Niger Delta region, Nigeria between the Latitude 04° 40' to 05 °55' N and Longitude 06° 50' to 07° 05' E (Bekwe, 2003) (Figure 1). The topography of River State is generally low-lying with heights of not more than 3 m above sea level and is generally covered by fresh water swamp, mangrove swamp, lagoonal marshes, tidal channels, beach ridges and sand bars (Dublin-Green et al., 1999). Its vegetation is an arcuate shaped basin with diverse vegetation which is characterized by 4 distinct ecological zones: coastal ridge barriers, brackish/freshwater swamp forests, mangrove forests and lowland rain forests, each of which offers diversity of setting for ecological resources and human activities (Odukoya, 2006; Onosode, 2003). Rivers State has an annual

ISSN 2054-6351 (print), ISSN 2054-636X (online)

rainfall of averages between 3,500 and 6,000 mm with the annual temperature range between 22 and 37 °C and a relative humidity of 75 % (UNEP, 2011). The chosen flaring sites and the sizes of the oil producing facilities within are Eleme Refinery I (1.6 by 1.1 km) and II (2.2 by 1.3 km) Petroleum Companies, Umurolu (4.2 by 2.4 km), Alua (170 by 90 m), Obigbo (650 by 650 m) and Chokocho (350 by 120 m) Flow Stations.

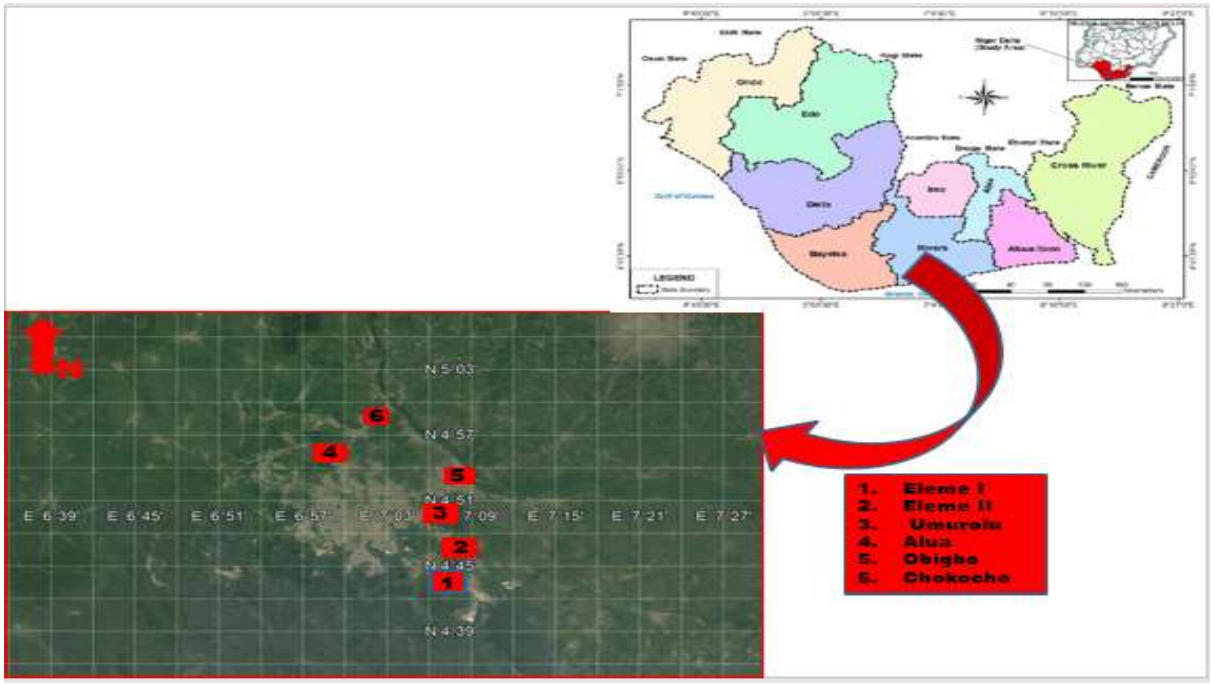

Figure 1: Gas flaring sites in Rivers State, Nigeria (Google Earth, 2019).

DATA SOURCES AND METHODOLOGY

Site selection

The criteria used for the selection of the flare sites used for this study are: 1) Availability of Landsat data in the U.S. Geological Survey (USGS)/National Aeronautics and Space Administration (NASA) Archive; 2) Function of the oil and gas facilities e.g. refineries, flow stations, terminals, oil wells; 3) Coverage i.e. availability of data covering the facility throughout the studyperiod; 4) Variety of size/capacity i.e. spatial dimensions of the facility (i.e. both largeand small facilities in order to compare their results); 5) Accessibility. Each flare site was investigated as a 12 by 12 km area (400 × 400 Landsat pixels); this size was chosen in order to include sufficient area for the change analysis of LC. This is based on previous literature by Dung et al. (2008) and Isichei and Sandford (1976), that the spatial extent of primary gas flare impacts was expected to be much less than 2 km in any direction.

Data used

In order to carry out detailed mapping of the LC at these sites, the two key data required for this study are satellite data and ground validation/fieldwork data. 15 scenes were downloaded from the U.S. Geological Survey Earth Resources Observation and Science (EROS) Data Centre website (http://earthexplorer.usgs.gov/) using the Glovis/Earth Explorer interface (Table 1). All the sites are located within a single Landsat scene (Path 188, Row 057), with the

ISSN 2054-6351 (print), ISSN 2054-636X (online)

results of the search being 3 Landsat 5 TM and 12 Landsat 7 ETM+ scenes from 17 January 1986 to 08 March 2013 (Table 1). The processing level for all the scenes is L1T, which means systematic radiometric and geometric correction using ground control points (GCPs), and the digital elevation model has been applied (Morakinyo, 2015). The problem of Scan Line Correction (SLC-off mode) with Landsat 7 sensor which started in 2003 that causes loss of part of data in the scenes from 2004 onward (Chen et al., 2012) was reduced to a minimum by setting one of the criteria for the selection of flare sites as the availability of data covering each site throughout the period of study. The 6 sites used for this study were successfully imaged for up to 96 % of the scenes used.

Table 1: Landsat 5 TM and Landsat 7 ETM+ used

S/N	Scene Identity No.	Date	UTC Time
1	LT51880571986017AAA07	17-01-1986	09:14
2	LT51880571986353XXX10	19-12-1986	09:04
3	LT51880571990356XXX03	22-12-1990	09:10
4	LE71880572000352EDC00	17-12-2000	09:35
5	LE71880572003360EDC01	26-12-2003	09:34
6	LE71880572005365ASN00	31-12-2005	09:34
7	LE71880572006352ASN00	18-12-2006	09:35
8	LE71880572007355ASN00	21-12-2007	09:35
9	LE71880572008326ASN00	21-11-2008	09:34
10	LE71880572009344ASN00	10-12-2009	09:36
11	LE71880572010347ASN00	13-12-2010	09:38
12	LE71880572011334ASN00	30-11-2011	09:38
13	LE71880572012033ASN00	02-02-2012	09:39
14	LE71880572012225ASN00	12-08-2012	09:40
15	LE71880572013067ASN00	08-03-2013	09:41

ISSN 2054-6351 (print), ISSN 2054-636X (online)

Methods for data processing

Steps used for the processing of Landsat 5 TM and Landsat 7 ETM+ data are: (1) Verification of geo-location points. 5 ground control points were selected over the Niger Delta using Google Earth. Four images for both Landsat 5 TM and Landsat 7 ETM+ were uploaded into ArcGIS and the selected GCPs were identified. The coordinates of these controls (obtained from both Google Earth and ArcGIS) were compared and a negligible difference found (1.0×10^{-6} to 7.3×10^{-6} m) (Table 2). This was taken as an acceptable error range for the geo-location of the imagery.

(2)The removal of zero or out of range values from the data and their replacement with not a number (nan) in order to avoid divide by zero errors in calculations. MATLAB code was used to process the data and to remove the zero and values at the upper and lower limits of the 8-bit data range which cannot be distinguished from noise. Noise results when the sensor is not sufficiently sensitive to resolve gradients in reflected or emitted radiation.

Table 2: Verification of geo-location points for Landsat 5 TM and Landsat 7 ETM+ data

Point	Google Earth Latitude (θ) Longitude (λ)	L5 TM & L7 ETM+ Latitude (θ) Longitude (λ)	Google Earth Eastings Northings	L5 TM & L7 ETM+ Eastings Northings	Remarks
A	4.410390 7.164627	4.410391 7.164548	296335 487741	296326 487741	A sharp bend on the ground
B	4.409837 7.139953	4.409910 7.140001	293596 487687	293601 487695	A point on top of the Liquefied Natural Gas (LNG) structure
C	4.428572 7.185888	4.428581 7.185897	298700 489746	298701 489747	A junction point on the ground
D	4.382893 7.172327	4.382890 7.172329	297182 484698	297183 484698	An edge of an LNG structure on the ground
E	4.426084 7.144811	4.426079 7.144809	294140 489482	294140 489482	An offshore point on an LNG terminal

(3) The radiometric calibration of the multispectral bands of the data. This was performed by converting the Digital Number (DN) values recorded by the remote sensor into top of atmosphere (TOA) radiance values based on sensor calibration parameters provided within the metadata files from USGS. This operation is carried out according to the Landsat 5 TM (Chander and Markham, 2003) and Landsat 7 ETM+ (NASA, 2002) Science Data Users Handbooks using equation.

$L_\lambda = ((LMAX_\lambda - LMIN_\lambda) / (QCALMAX - QCALMIN)) \times (QCAL\text{-}QCALMIN) + LMIN_\lambda$ (1)

Where:

ISSN 2054-6351 (print), ISSN 2054-636X (online)

L_λ= Spectral Radiance at the sensor's aperture in $Wm^{-2}sr^{-1}\mu m^{-1}$;
QCAL = the quantized calibrated pixel value in DN (Digital Number);
$LMIN_\lambda$= the spectral radiance that is scaled to QCALMIN in $Wm^{-2}sr^{-1}\mu m^{-1}$;
$LMAX_\lambda$= the spectral radiance that is scaled to QCALMAX in $Wm^{-2}sr^{-1}\mu m^{-1}$;
QCALMIN = the minimum quantized calibrated pixel value (corresponding to $LMIN_\lambda$) in DN = 1 for LPGS (a processing software version) products;
QCALMAX = the maximum quantized calibrated pixel value (corresponding to $LMAX_\lambda$) in DN = 255

(4) Computation of TOA reflectance for multispectral bands 1 to 4, including the application of simple Sun angle correction using equation 2.

$$\rho p = (\pi \times L\lambda \times d^2) \div (ESUN\lambda \times \cos \theta s) \quad (2)$$

Where:
ρp = Unitless effective at-satellite planetary reflectance;
L is measured per unit solid angle;
πL = Upwelling radiance over a full hemisphere;
d = Earth-Sun distance in astronomical units
$ESUN\lambda$ = Mean solar exoatmospheric irradiances.
θs = Solar zenith incident angle in degrees (Chander and Markham, 2003).

(5) Correction for the atmospheric effects for the multispectral bands (1-4) to retrieve the real surface parameters by removing the atmospheric effects, such as (potentially) thin clouds (Inamdar et al., 2008), molecular and aerosol scattering, absorption by gases (such as water vapour, ozone, oxygen) and aerosol, and sometime also the correction for cloud shadows, upward emission of the radiation from the Earth surface (Qin et al., 2011), environmental radiance which produces the adjacency effects, variation of illumination geometry including the Sun's azimuth and zenith angles, and ground slope (Mather, 2004). Accordingly, the visible bands of Landsat 5 TM and Landsat 7 ETM+ are more strongly affected by varying atmospheric conditions than the infrared and mid-infrared bands. Atmospheric correction consists of two major steps: parameter estimation and surface reflectance retrieval (Liang et al., 2001). The most difficult component of atmospheric correction is to eliminate the effect of aerosols. The fact that most aerosols are often distributed heterogeneously makes this task more difficult (Liang et al., 2001).

The methods reported in the literature for the quantitative atmospheric correction of Landsat 5 TM and Landsat 7 ETM+ imagery visible and NIR bands can be roughly classified into the following groups: Invariant-object, histogram matching, dark object subtraction (DOS), and contrast reduction (Liang et al., 2001). DOS method have a long history (Kaufman et al., 2000; Liang et al., 1997; Teillet and Fedosejevs, 1995) and are probably the most popular atmospheric correction method (Liang et al., 2001) reported in the literature. The basic assumption is that within the image some pixels are in complete shadow and their radiances received at the satellite are due to the atmospheric scattering (path radiance). This assumption is combined with the fact that very few targets on the Earth's surface are absolute black, so an assumed 1 % minimum reflectance is better than 0 % (Chavez, 1996). Both MODIS and medium resolution imaging spectroradiometer (MERIS) atmospheric correction algorithms

ISSN 2054-6351 (print), ISSN 2054-636X (online)

(Santer et al., 1999) are based on this principle. However, this method assumes that this error is the same over the whole image (Liang et al., 2001).

For this study, DOS method was used and its principle applied to this study means that pixels corresponding to the darkest location (Atlantic Ocean) were selected for each band 1 to 4 (Table 3). The number of pixels obtained varies depending on the size of the darkest spot. The reflectance for these dark pixels was computed for each band and the minimum value obtained for each band was used as an estimate of the atmospheric reflectance for the respective band. These small errors were subtracted from the computed reflectance for each pixel of the whole image to reduce the atmospheric effects.

Table 3: Latitude and Longitude of some dark pixels over Atlantic Ocean

Image ID	Band 1 (Lat. /Long.)	Band 2 (Lat. /Long.)	Band 3 (Lat. /Long.)	Band 4 (Lat. /Long.)
LT51880571986 017AAA04	4.336699 7.250121	4.332076 7.257068	4.336710 7.254742	4.327437 7.257078
LT51880571987 004XXX04	4.169107 7.074345	3.798029 7.699768	3.792277 7.694059	3.788445 7.690256
LT51880571986 353XXX10	4.281913 7.366087	4.183774 7.659434	4.138324 7.352093	4.076853 7.143137
LE71880571999 333AGS00	3.665176 6.592174	3.665176 6.592174	3.723996 6.567263	3.664760 6.592157
LE71880572000 352EDC00	4.281250 8.164940	4.282325 8.163866	4.281548 8.164345	4282569 8.163037
LE71880572003 008SGS00	3.591636 7.948805	3.594024 7.948802	3.598809 7.948797	3.596421 7.948800

Land cover mapping and classification

The accuracy of LULC classification are of great significance to global change, environmental monitoring etc. (Yuechen et al., 2012). However, there is no uniform standard for LULC classification at present, which brings a lot of inconvenience to the collection and analysis of LC data (Yue et al., 2018). Several researchers have worked on LULC analysis using different methods to achieve their results. For example, Aixia et al. (2006) applied fuzzy K-means non-supervised classifier to get 4 classes of the LC. Yuechen et al. (2012) adopted supervised digital classification using maximum likelihood classifier for identifying 8 classes of LULC. Maaharjan (2018) adopted interactive supervised image classification system to obtain 4 classes. Kayet et al. (2018) and Fonteh et al. (2016) employed Support Vector Machine (SVM) method for separation of 10 LULC classes (water, settlement, bare ground, dark mangroves, green mangroves, swampy vegetation, rubber, coastal forest and other vegetation and palms) (Fonteh et al., 2016). SVM is more advantageous in object-based classification and image analysis (Tan and Zhang, 2008; Tzotsos and Argialas, 2008).

ISSN 2054-6351 (print), ISSN 2054-636X (online)

A stochastic model was combined with visual interpretation to estimate and evaluate the change detection for 3 classes (Yuechen et al. (2012) of LC (Built up, non- urban and water bodies) (Pareta, 2014). In addition, Chen and Li (2004) applied Soil and Water Assessment Tool (SWAT) model to simulate different LC. Furthermore, Niehoff et al. (2002) used LU change modelling kit (LUCK) with a modified version of the physically-based hydrological model WaSiM-ETH for flood prediction. Tomar et al. (2017) used image processing method in ERDAS imagine and ArcGIS 10.3 for detection of 5 classes of LULC changes. Boori and Voženílek (2014) adopted object-oriented classification method for 3 classes of LC. In addition, 5 LULC classes namely built up, agriculture land, open space, vegetation and water body were identified by Shravya and Sridhar (2017).

For this study, the first unsupervised cluster analysis (Alvarez, 2009; Hestir et al., 2008) of the atmospherically corrected reflectance (bands 1-4) using the K-means function (Şatır and Berberoğlu., 2012; Hestir et al., 2008) of the MATLAB tool was carried out. The results obtained give 3 classes of LC type with cloud classified as the 4^{th} class. The 4 classes identified are any of these 3: vegetation, water, soil and built up area, and cloud as the 4^{th} class. The next stage was the elimination of the class for the cloud by masking using MATLAB code. The second cluster analysis was performed with the cloud-masked reflectance (bands 1-4) to give 4 (Maaharjan, 2018; Boori et al., 2015) (vegetation, soil, built up area and water) LC types for all sites. Landsat Short Wave Infra-Red (SWIR) bands 5 and 7 were also employed for the classification of LC types but they could not give useful information as bands 1-4 hence, they were dropped for further analysis. LC types at these flaring sites change from scene to scene and from site to site. Furthermore, through visit to the Niger Delta, fieldwork observation and measurements for ground validation of Landsat 5 TM and Landsat 7 ETM+ took place at Eleme Refinery I and II in August and September, 2012, during a period of six weeks. It was confirmed that LC types at these flaring sites are vegetation, some buildings, open land i.e. bare soil and water bodies. Also, LC types for other 4 flaring sites are similar to that of Eleme Refinery I and II because the topography of the Niger Delta is the same. A summary of stages in the Landsat 5 TM and Landsat 7 ETM+ data processing is shown in the schematic diagram (Figure 2).

ISSN 2054-6351 (print), ISSN 2054-636X (online)

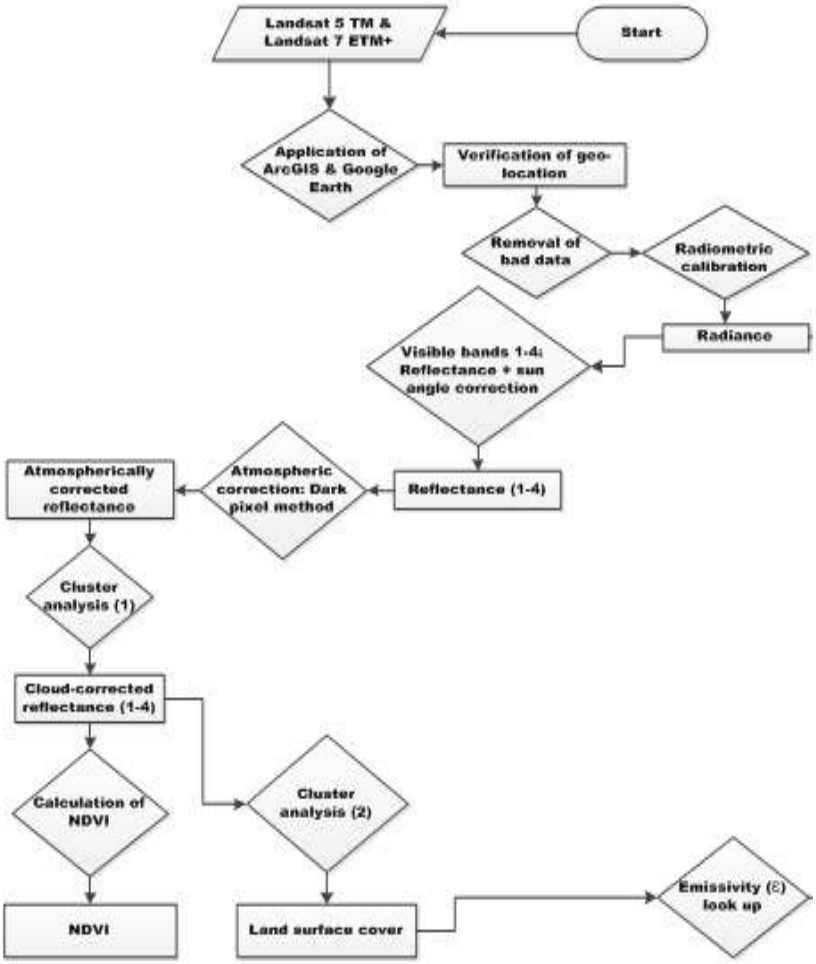

Figure 2: Schematic diagram for the processing of Landsat 5 TM and Landsat 7 ETM+ for mapping and classification of land cover types at flaring sites in the Niger Delta.

Estimation of Emissivity value

For this research, the method used to estimate Ɛ value for LC types at the 6 flaring sites is based on the Ɛ of 4 LC types (vegetation, soil, built up areas and water) present at each site. Each pixel LC types were considered for the entire site and their Ɛ values (both minimum and maximum) were taken from the literature. Mean of Ɛ value for LC types for each single pixel obtained from using their minimum and maximum values from the literature were calculated. Average of these 2 results of Ɛ values i.e. $Ɛ_{min}$ and $Ɛ_{max}$ were obtained for each pixel and the same procedure was repeated for all pixels in the selected 12 by 12 km area around the gas flare source. Therefore, the Ɛ value for each 30 m² Landsat pixel is a combination of the Ɛ value of background features and that of any flare present within the pixel. The authors adopted an independent method of using LC types at each site for the correction of Ɛ value rather than Global Land Cover (GLC) data from USGS in order to ensure quality control primarily. Table 4 is the look up table (LUT) for the Ɛ value of LC types and gas flare.

ISSN 2054-6351 (print), ISSN 2054-636X (online)

Table 4: Surface emissivity for land cover types and gas flares

Land cover type	Emissivity value (minimum)	Emissivity value (maximum)	Reference
Vegetated areas:			
Short grass	0.979	0.983	Labed and Stoll, 1991
Bushes (≈ 100 cm)		0.994	Labed and Stoll, 1991
Densely vegetated areas	0.960	0.980	Jin and Liang, 2006
Soils:			
Bare soil		0.960	Humes et al., 1994
Bare soil (desert)		0.900	Jin and Liang, 2006
Bare soil (sandy)		0.930	Hipps, 1989
Bare soil (loamy sand)		0.914	van de Griend et al., 1991
Water body:			
Water body	0.950	0.980	Masuda et al., 1988
Water body		0.990	Stathopoulou and Cartalis, 2007
Built up areas:			
Medium built		0.964	Stathopoulou and Cartalis, 2007
Densely urban		0.946	Stathopoulou and Cartalis, 2007
Flare:			
	0.13	0.40	Shore, 1996
	0.15	0.30	PTT, 2008
	0.18	0.25	Sáez, 2010

RESULTS/ FINDINGS

Land cover types

In order to achieve the aim of this study, the following analysis steps were used for the classification and ascertaining of LC types at these flaring sites: an overview of spatial variability in land use that was achieved using simple visual examination of Worldview-1 and 2 and IKONOS pseduo-true colour images accessed through Google Earth and Digital Global (http://browse.digitalglobe.com/imagefinder/public.do). The LC classification results were used to summarise the LC types around each site. Then, the Landsat reflective bands were examined to identify any unusual ground features associated. Finally, the pseudo-true colour images from the combination of bands 3, 2 and 1 as red, green and blue (RGB) were included as a comparison to the higher spatial resolution WorldView and IKONOS browse images in identifying features at each site (the green features in the Landsat RGB image should correspond to green features in Google Earth) (Figures 3-8). Other Landsat bands combination such as Red, Green and Near Infrared bands; Green, Blue and Near Infrared; Red, Green and Short-Wave Infrared (band 5) and Red, Green and Short-Wave Infrared (band 7) were also

ISSN 2054-6351 (print), ISSN 2054-636X (online)

processed to obtain their pseudo-true colour images. The combination of RGB bands gives the best result and so it was used for the qualitative analysis of this study.

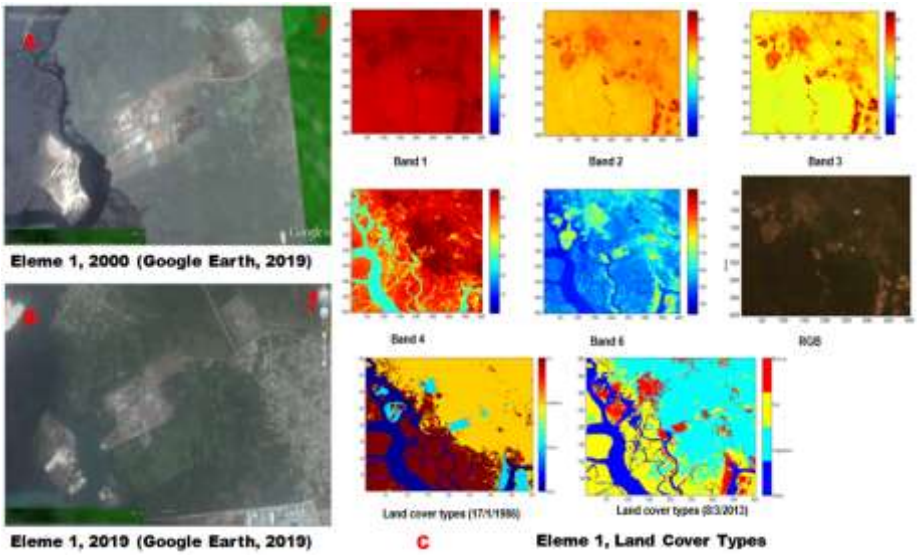

Figure 3: Eleme Refinery I Petroleum Company site: A) in 2000; B) in 2019; C) Bands 1-4, 6, RGB (8/3/2013) and land cover types (17/1/1986 & 8/3/2013), (X and Y axes: pixel numbers; scale bar: digital number, DN)

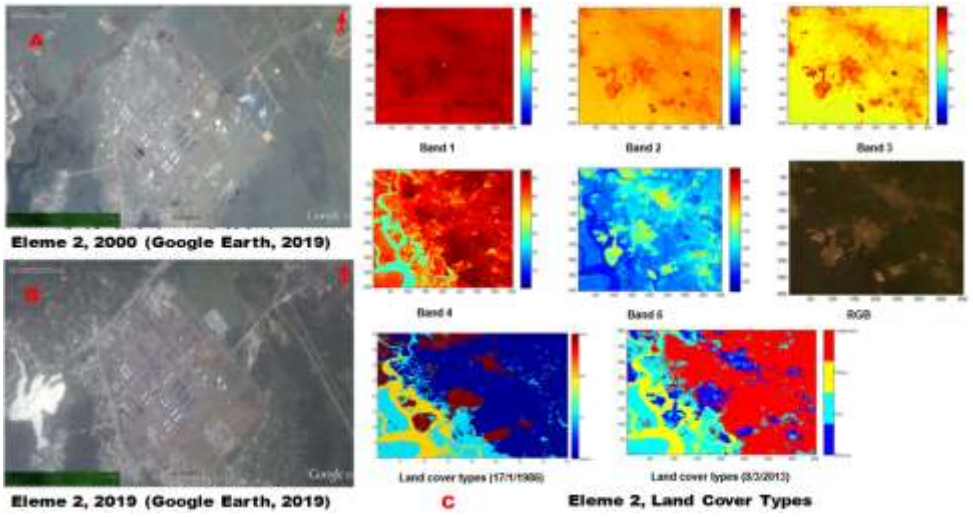

Figure 4: Eleme Refinery II Petroleum Company site: A) in 2000; B) in 2019; C) Bands 1-4, 6, RGB (8/1/2013) and land cover types (17/1/1986 & 8/3/2013), (X and Y axes: pixel numbers; scale bar: digital number, DN)

ISSN 2054-6351 (print), ISSN 2054-636X (online)

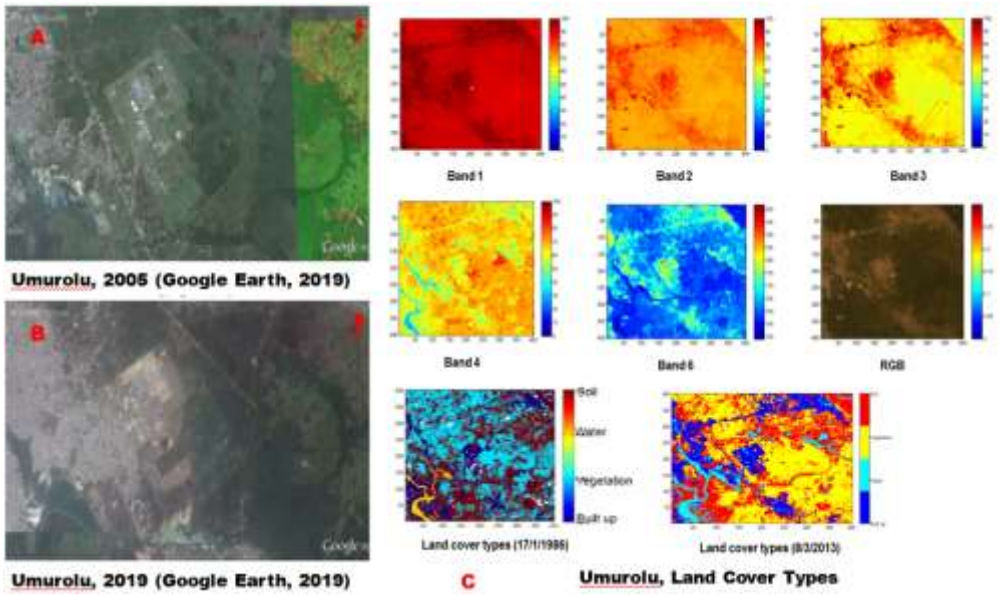

Figure 5: Umurolu Flow Station site: A) in 2005; B) in 2019; C) Bands 1-4, 6, RGB (8/3/2013) and land cover types (17/1/1986 & 8/3/2013), (X and Y axes: pixel numbers; scale bar: digital number, DN)

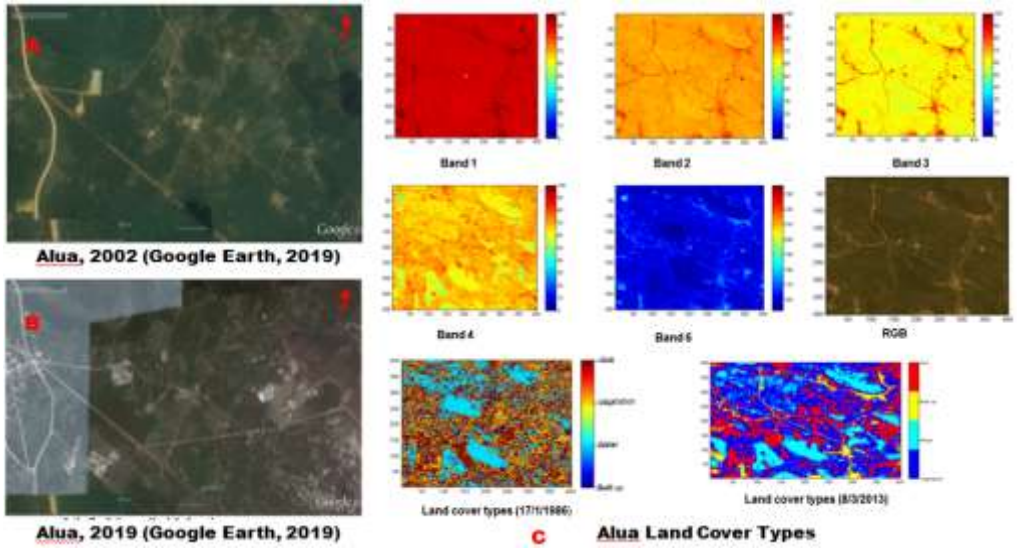

Figure 6: AluaFlow Station site: A) in 2002; B) in 2019; C) Bands 1-4, 6, RGB (8/3/2013) and land cover types (17/1/1986 & 8/3/2013), (X and Y axes: pixel numbers; scale bar: digital number, DN)

ISSN 2054-6351 (print), ISSN 2054-636X (online)

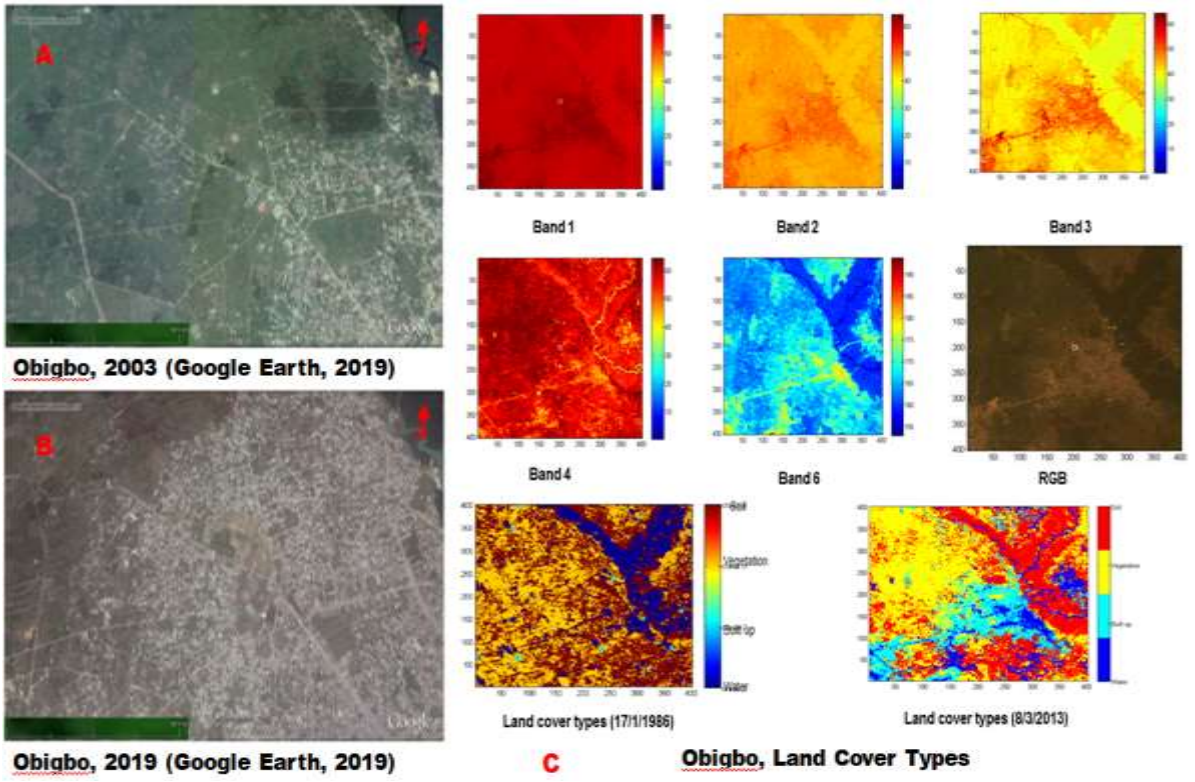

Figure 7: Obigbo Flow Station site: A) in 2003; B) in 2019; C) Bands 1-4, 6, RGB (8/3/2013) and land cover types (17/1/1986 & 8/3/2013), (X and Y axes: pixel numbers; scale bar: digital number, DN)

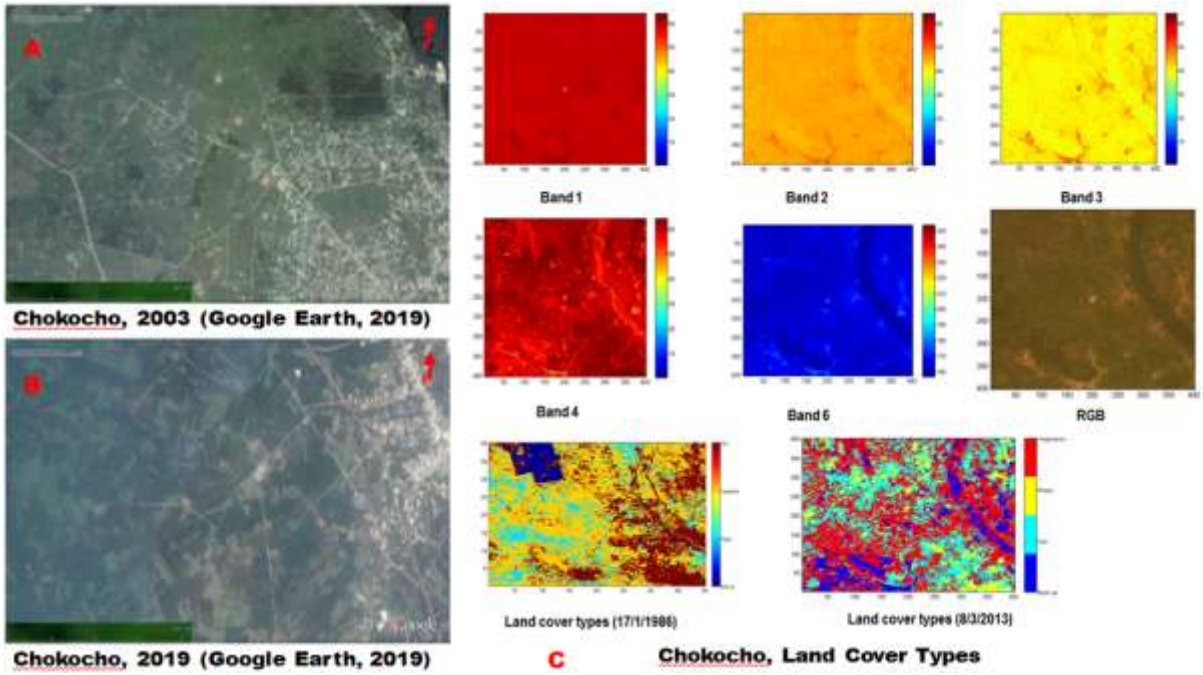

Figure 8: Chokocho Flow Station site: A) in 2003; B) in 2019; C) Bands 1-4, 6, RGB (8/3/2013) and land cover types (17/1/1986 & 8/3/2013), (X and Y axes: pixel numbers; scale bar: digital number, DN)

ISSN 2054-6351 (print), ISSN 2054-636X (online)

Figures 3 A & B shows that there is infrastructural development and great expansion of built up such as buildings and road networks toward the North-West, East and spreading toward East-South and East-North of the Eleme Refinery I site from 1986 to 2019; construction of roads at the North-East side and across the river has taken place in Figures 3 C and LC types of 8/3/2013. These leads to reduction on bear soil and vegetation cover. Figures 4 A, B & C shows the state of Eleme Refinery II site in 1986, 2000, 2013 and 2019 with developmental growth in number of built up around the refinery that spread toward West, South-West in 2019 compared to 2000; its LC map (8/3/2013) shows the increase in built up area such as buildings, roads that were not available in 1986. These have caused reduction in bare soil and vegetation cover within the site. For Umurolu site (Figures 5 A, B & C), there is an increase in built up area around the flow station and massive infrastructural development due to human settlements towards the West, North-West and South-West of the site on LC map (8/3/2013) and the Google Earth image of 2019 that were not present on LC map (17/1/1986) and the Google Earth image of 2005. This size of soil and vegetation cover has been greatly reduced.

Figures 6 A, B & C shows that in 2013 and 2019 there are more built up areas at the West and South-East areas of Alua site as compared to 1986; in LC map (17/1/1986), a portion of the site towards North-East and East-South with soil and vegetation have been replaced with water in 8/3/2013. In addition, some portions of the site from the centre toward North and spread towards North-East that were covered with water in 17/1/1986 map have been replaced with vegetation in 8/1/2013 map. Roads are presented at the North-East, South-West and almost diagonally from the South-East to the North-East of the site in 8/3/2013 map. Figures 7 A, B & C show the explosive urban growth of built up e.g. several houses and route networks at Obigbo site in 2013 towards 2019 as compared to 1986.

There is massive settlement at the centre of the site, spreading toward South-East, South, South-West in 8/3/2013 map but not available in 17/1/1986 map. There is also, built up development at the North, towards North-East after the river in 8/3/2013 map that is not shown in 17/1/1986 map. In 17/1/1986 map, the width of the flowing river is wider while it has been narrowed in 8/3/2013 map. There are significant reduction changes in soil and vegetation cover in 2013 towards 2019 compared to 1986. For Chokocho, Figures 8 A, B & C shows a large building at the North-West of the site in 1986 which is no more in 2013. Growth in the settlement at the East, South and South-West of the site is shown in 8/3/2013 map. There is also a road development linked North-East to the East in 8/3/2013 map while it was not available in 17/1/1986 map. Generally, the influence of the activities of crude oil production and refining, infrastructural development and other human activities including farming, logging etc. have change LC at all sites, affects LC negatively and causes degradation of the ecosystem.

ISSN 2054-6351 (print), ISSN 2054-636X (online)

Estimation of Emissivity value

The Ɛ results (Table 5) from LC types at each flaring site are obtained from 1 season (dry) out of 2 seasons (rain and dry) available in Nigeria. The emissivity value recorded for vegetation, built up, water and soil at each site vary from 1986 to 2013. Since Ɛ is strongly dependent on LULC types (Mallick et al., 2012), this study applied Ɛ values to evaluate the % of LC loss for the 4 LC types available at the sites investigated. Generally, the Ɛ values obtained for 4 LC types for all sites in 1986 is higher than those obtained in 2013. In 1986, vegetation cover has the highest Ɛ values throughout the entire 6 sites, followed by water. In 2013, the Ɛ values recorded for the same 4 LC within the sites have been greatly reduced. Table 6 shows the difference in Ɛ values (%) obtained in 1986 and that of 2013 for 6 sites investigated. The % of vegetation cover loss for all sites shows Obigbo site is with the highest (8.8 %) and Eleme I site is with the lowest (3.2 %). The % of increase in built up LC also shows Obigbo site having the highest (6.3 %) while both Eleme I and II gives the lowest (3.3 %). Eleme II has the highest % of water LC loss (6.0 %) while Umurolu site shows the lowest (3.5 %). For soil LC, Alua site has the highest % of loss (7.3 %) while Eleme II recorded the lowest (3.7 %). In summary, the % of LC loss recorded could be attributed to the impact of crude oil production and refining activities, infrastructural development and other human activities such as farming, logging etc.

ISSN 2054-6351 (print), ISSN 2054-636X (online)

Table 5: Emissivity results for the flaring sites in the Niger Delta from 1986 to 2013

Flaring sites	**17/1/1986**				**19/12/1986**				**22/12/1990**				**17/12/2000**			
	Veg.	**Built**	**Water**	**Soil**	**Veg.**	**Built**	**Water**	**Soil**	**Veg.**	**Built**	**Water**	**Soil**	**Veg.**	**Built**	**Water**	**Soil**
Eleme I	0.979	0.964	0.970	0.960	0.962	0.903	0.951	0.962	0.981	0.967	0.961	0.965	0.973	0.960	0.952	0.970
Eleme II	0.980	0.953	0.980	0.930	0.965	0.900	0.977	0.910	0.962	0.962	0.981	0.960	0.960	0.948	0.980	0.940
Umurolu	0.980	0.954	0.950	0.972	0.980	0.902	0.945	0.966	0.970	0.945	0.955	0.961	0.981	0.968	0.955	0.936
Alua	0.999	0.962	0.980	0.980	0.979	0.968	0.980	0.901	0.973	0.942	0.980	0.902	0.980	0.956	0.982	0.901
Obigbo	0.988	0.963	0.970	0.974	0.983	0.965	0.957	0.944	0.933	0.951	0.965	0.934	0.912	0.961	0.898	0.910
Chokocho	0.993	0.946	0.980	0.963	0.994	0.948	0.981	0.930	0.996	0.954	0.978	0.943	0.984	0.966	0.985	0.940
	26/12/2003				**31/12/2005**				**18/12/2006**				**21/12/2007**			
Eleme I	0.981	0.487	0.965	0.967	0.981	0.961	0.945	0.969	0.971	0.964	0.948	0.960	0.983	0.943	0.968	0.961
Eleme II	0.963	0.968	0.984	0.901	0.960	0.953	0.980	0.900	0.968	0.921	0.981	0.920	0.965	0.965	0.988	0.970
Umurolu	0.984	0.961	0.951	0.960	0.982	0.954	0.956	0.967	0.980	0.946	0.951	0.977	0.923	0.937	0.955	0.961
Alua	0.979	0.934	0.980	0.900	0.984	0.962	0.981	0.901	0.979	0.912	0.960	0.923	0.979	0.966	0.978	0.905
Obigbo	0.891	0.956	0.920	0.981	0.931	0.963	0.945	0.900	0.983	0.900	0.910	0.940	0.912	0.953	0.931	0.891

ISSN 2054-6351 (print), ISSN 2054-636X (online)

Chokocho	0.994	0.949	0.980	0.930	0.984	0.946	0.958	0.934	0.964	0.902	0.982	0.936	0.964	0.956	0.978	0.983
	21/11/2008				**10/12/2009**				**13/12/2010**				**30/11/2011**			
Eleme I	0.970	0.967	0.948	0.962	0.982	0.946	0.967	0.965	0.982	0.961	0.961	0.977	0.971	0.963	0.975	0.960
Eleme II	0.952	0.962	0.978	0.960	0.973	0.942	0.980	0.906	0.969	0.968	0.985	0.968	0.968	0.946	0.981	0.963
Umurolu	0.984	0.945	0.920	0.961	0.981	0.932	0.975	0.936	0.981	0.966	0.950	0.960	0.980	0.956	0.943	0.926
Alua	0.980	0.942	0.956	0.942	0.979	0.964	0.981	0.920	0.979	0.956	0.978	0.958	0.979	0.946	0.984	0.942
Obigbo	0.980	0.951	0.910	0.921	0.930	0.954	0.950	0.904	0.900	0.966	0.910	0.912	0.947	0.964	0.950	0.890
Chokocho	0.994	0.954	0.965	0.930	0.974	0.964	0.968	0.940	0.952	0.934	0.978	0.943	0.984	0.964	0.973	0.982
	02/02/2012				**12/08/2012**				**08/03/2013**							
Eleme I	0.971	0.946	0.955	0.962	0.971	0.964	0.965	0.964	0.947	0.931	0.942	0.923				
Eleme II	0.966	0.946	0.980	0.918	0.961	0.921	0.968	0.929	0.941	0.920	0.920	0.900				
Umurolu	0.985	0.945	0.965	0.936	0.928	0.946	0.945	0.944	0.935	0.920	0.915	0.931				
Alua	0.971	0.942	0.981	0.903	0.979	0.912	0.960	0.942	0.959	0.902	0.938	0.907				
Obigbo	0.972	0.942	0.899	0.914	0.925	0.900	0.932	0.908	0.900	0.900	0.931	0.911				
Chokocho	0.991	0.923	0.982	0.936	0.984	0.902	0.985	0.973	0.945	0.901	0.935	0.902				

ISSN 2054-6351 (print), ISSN 2054-636X (online)

Table 6: Difference in Ɛ values (%) between 1986 & 2013 for the study sites

Sites	Vegetation (%)		Builtup (%)		Water (%)		Soil (%)	
Eleme I	0.032	3.2	0.033	3.3	0.038	3.8	0.037	3.7
Eleme II	0.039	3.9	0.033	3.3	0.060	6.0	0.030	3.0
Umurolu	0.045	4.5	0.034	3.4	0.035	3.5	0.041	4.1
Alua	0.040	4.0	0.060	6.0	0.042	4.2	0.073	7.3
Obigbo	0.088	8.8	0.063	6.3	0.039	3.9	0.063	6.3
Chokocho	0.048	4.8	0.045	4.5	0.045	4.5	0.061	6.1

DISCUSSION

The nature of LULC change refers to what is changing and to what is changing to (Mmon and Fred-Nwagwu, 2013). This change is due to human activities in the area because land is one of the most important natural resources on which human depend for livelihood. The LULC pattern of an area is an outcome of natural and socio-economic factors and their utilization by man in time and space (Ademiluyi et al., 2008). The information about the nature of change serves as a vital tool in decision making; the nature of LULC change shows the direction of change. For the 6 sites studied, the changes in LC differ due to different human activities including gas flaring within each site which is supported by (Mmon and Fred-Nwagwu, 2013; and Ademiluyi et al., 2008). The use of Google Earth images (Tomar et al., 2017), Landsat reflective bands and the pseudo-true colour images from the combination of bands 3, 2 and 1 (RGB) helps to clarify features within each site but does not allow the choice of a specific feature from the main feature of the numerous features (Carleer and Wolff, 2006).

Generally, human settlements, infrastructural development such as roads construction and the impact of oil and gas facilities are the major causative agent of LC change in these sites. Furthermore, the Ɛ values estimated for the 4 LC types for the 6 sites are not stable but changing from 1986 to 2013. This is supported by Mallick et al. (2012) who stated that Ɛ has strong LULC dependence.

Furthermore, the results of LC change analysis and Ɛ shows the extent of changes in LC and damages done to land due to human activities, infrastructural development, and exploitation and refining activities for oil and gas at these sites. The study suggests that by using medium resolution satellite data (Landsat 5 TM and Landsat 7 ETM+) with K-mean MATLAB tool a spatial data base can be generated for the Niger Delta region (Nigeria) to assess the LULC. Based on these data sets, monitoring and management of both the urban and rural areas can be done easily and in a more meaningful way (Rahman et al., 2012). Furthermore it can become a policy tool for Government officials and urban planners to control and manage unplanned LULC change; and to enforce regulations that will reduce degradation of the environment to the minimum. In addition, the results of Ɛ values obtained in this study is closing the gap between Nigeria and the rest of the world on the reseaches relating to Ɛ by providing the literature on the topic of Ɛ for the Niger Delta. The Ɛ values obtained will serve as a basis for other future researchers to use for studies on Ɛ values, retrieval of Land Surface Temperature (LST) etc. for the Niger Delta.

ISSN 2054-6351 (print), ISSN 2054-636X (online)

CONCLUSION

This study illustrates the use of RS and K-mean of MATLAB tool as important technologies for extracting LULC which can be very challenging with the use of conventional mapping techniques. Assessment of environment is made possible by these technologies in less time, at low cost and with better accuracy. The results of LC classification obtained shows that the adopted K-means method can distinguish up to 4 LC types very well in the Niger Delta. Changing in LC types for all the 6 sites is caused by human activities including farming, logging, infrastructural developments, and the effects of oil and gas production and refining activities. This also led to variation in the Ɛ values recorded throughout the period. The LC changes and Ɛ values recorded in this research will serve as a basis to understand the patterns and possible consequences of LC changes and Ɛ values in the Niger Delta. In addition, this study will help to develop new comparative research on the pattern and processes of LC change in the Niger Delta region and Northern Nigeria; and also to use data from the 2 seasons (dry and rain) available in Nigeria. Therefore, there is a need for proper land use planning and enforcement of development control to forestall the negative socio-economic impacts of LULC changes. Nigerian Government should provide incentives that move individuals from conflicting relations with their natural system, toward more sustainable landscape transitions; and there should be the regulatory presence of Nigerian Government (e.g. a ban on logging). Finally, the future research should pay more attention to the LULC driving factors of social economy and the natural environment; economic development and technological advancement; and the exploration of the environmental change effects caused by LULC.

REFERENCE

Ademiluyi, I. A., Okude, A. S and Akanni, C. O. (2008): "An appraisal of land use and land cover mapping in Nigeria". African Journal of Agricultural Research 3 (9): 581-586.

Agoha, S. C. (2009): "Analysis of rural-urban land use change in Umuahia, South Eastern Nigeria". Unpublished M.Sc. Dissertation submitted to Department of Geography and Environmental Management University of Abuja.

Aixia, L., Jing, W. and Chunyan, L. V. (2006). "Land cover classification based on MODIS data in area to the North-West of Beijing". Progress in Geography 02.

Alvarez, J. (2009). "Land cover verification along Freeway Corridors, Natomas Basin Area, California, USA". [Online]. Available: http://www.academic.emporia.edu/aberjame/student/alvarez4/natchange.htm l [Accessed 26th September 2016].

Antonarakis, A. S., Richards, K. S and Brasington, J. (2008). "Object-based land cover classification using airborne LiDAR". Remote Sensing of Environment 112(6): 2988-2998.

Awoniran, D. R., Adewole, D., Adegboyega, S. S and Anifowose, Y. (2013). "Assessment of environmental responses to land use/land cover dynamics in the lower Ogun River Basin, South-Western Nigeria". International Journal of Sustainable Land Use and Urban Planning. ISSN 1927-8845 1(2): 16-31.

Becker, F and Li, Z. L. (1995). "Surface temperature and emissivity at various scales: definition, measurement and related problems". Remote Sensing Reviews 12: 225-253.

ISSN 2054-6351 (print), ISSN 2054-636X (online)

Bekwe, W. F. (2003). "Urban flood hazards mapping; A GIS approach: A case study of Port Harcourt". Unpublished M.Sc. Dissertation, University of Ibadan, Ibadan.

Bernard, A. C and Wilkinson, G. G. (1997). "Training strategies for neural network soft classification of remotely-sensed imagery". International Journal of Remote Sensing 8(8): 1851-1856.

Boori, M. S and Voženílek, V. (2014). "Remote sensing and land use/land cover trajectories. Journal of Geophysical Remote Sensing 3: 123. doi:10.4172/2169-0049.1000123.

Boori, M. S., Vozenílek, V., Balzter, H and Choudhary, K. (2015). "Land surface temperature with land cover classes in ASTER and Landsat Data". Journal of Geophysics and Remote Sensing 4(1), http://dx.doi.org/10.4172/2169- 0049.1000138.

Braimoh, A. K and Vlek, P. L. G. (2004). "Land cover change analyses in the Volta Basin of Ghana". Earth Interact. 8:1-17.

Carleer, A. P and Wolff, E. (2006). "Urban land cover multi-level region-based classification of VHR data by selecting relevant features". International Journal of Remote Sensing 27(6): 1035-1051.

Caselles, V and Sobrino, J. A. (1989). "Determination of frosts in orange groves from NOAA-9 AVHRR data". Remote Sensing of Environment 29: 135-146.

Chander, G and Markham, K. (2003). "Revised Landsat-5 TM radiometric calibration procedures and post calibration dynamic ranges". IEEE Transactions on Geoscience and Remote Sensing 41(11): 2674-2677.

Chavez, P. S. (1996). "Image-based Atmospheric Corrections-Revisited and Improved". Photogrammetry Engineering and Remote Sensing 62(9): 1025-1036

Chen, J. F, Li, X. B. (2004). "Simulations of hydrological response to land cover changes". Chinese Journal of Applied Ecology. 15: 833-836.

Chen, F., Zhao, X and Ye, H. (2012). "Making use of the Landsat 7 SLC-off ETM+ image through different recovering approaches". Postgraduate Conference on Infrastructure and Environment (3rd IPCIE), (2): 557-563. [Online]. Available: http://dx.doi.org/10.5772/48535 [Accessed 26th September 2014].

Desanker, P. V., Frost, P. G. H., Justice, C. O and Scholes, R. J. (1997). "The Miombo Network: Frameworks for a terrestrial transect study of land use and land cover change in the Miombo ecosystems of Central Africa". IGBP Report 41.

Dublin-Green, C. O., Awosika, L. F and Folorunsho, R. (1999). "Climate variability research activities in Nigeria". Nigerian Insitute for Oceanography and Marine Research, Victoria Island, Lagos, Nigeria.

Dung, E. J., Bombom, L. S and Agusomu, T. D. (2008). "The effects of gas flaring on crops in the Niger Delta, Nigeria". GeoJournal 73: 297-305.

Ejaro, S. P. (2008): "Analyses of Land use and land cover change in the Federal Capital Territory (FCT), Abuja using Multi-Temporal Satellite Data". Unpublished Ph.D Thesis, Department of Geography and Environmental Management, University of Abuja, Nigeria.

Fasona, M. J and Omojola, A. S. (2005). "Climate change, human security and communal clashes in Nigeria". Paper presented at an International Workshop on Human Security and Climate Change, Asker, Norway, 21-23.

Fonteh, M. L., Theophile, F., Cornelius, M. L., Main, R., Ramoelo, A and Cho, M. A. (2016). "Assessing the utility of Sentinel-1 C Band Synthetic Aperture Radar Imagery for land

ISSN 2054-6351 (print), ISSN 2054-636X (online)

use land cover classification in a tropical coastal system When Compared with Landsat 8. Journal of Geographic Information System 8: 495-505.

Foody, G. M. (2002). "Status of land cover classification accuracy assessment". Remote Sensing of Environment 80 (1): 185-201.

Forkuo, E. K and Adubofour, F. (2012). "Analysis of forest cover change detection". International Journal of Remote Sensing Applications 2(4): 82-92.

Gillespie, A., Rokugawa, S., Matsunaga, T., Cothern, J. S., Hook, S and Kahle, A. B. (1998). "A temperature and emissivity separation algorithm for Advanced Spaceborne Thermal Emission and Reflection Radiometer (ASTER) images". IEEE Transactions on Geoscience and Remote Sensing 36 (4): 1113-1126.

Gong, P., et al. (2006). "Progress of the research on classification system of land vegetation". China Journal of Agricultural Resources and Regional Planning 27(2): 35-40.

Hegazy, I. R and Kaloop, M. R. (2015). "Monitoring urban growth and land use change detection with GIS and remote sensing techniques in Daqahlia Governorate Egypt". International Journal of Sustainable Built Environment 4(1): 117-124.

Hestir, E. L., Khanna, S., Andrew, M. E., Santos, M. J., Viers, J. H., Greenberg, J. A., Rajapakse, S. S and Ustin, S. L. (2008). "Identification of invasive vegetation using hyperspectral remote sensing in the California Delta ecosystem". Remote Sensing of Environment 112: 4034-4047.

Hipps, L. E. (1989). "The infrared emissivities of soil and Artemisia tridentate and subsequent temperature corrections in a shrub-steppe ecosystem". Remote Sensing of Environment 27: 337-342.

Hua, W., Chen H and Sun S. (2015). "Assessing climatic impacts of future land use and land cover change projected with the CanESM2 model". International Journal of Climatology 35(12): 3661-3675.

Huajun, T. (2009). "Research progress of land use/land cover change (LUCC) model". Journal of Geography 64(4): 456-468.

Hu, Q., Willson, G. D., Chen, X and Akyuz, A. (2005). "Effects of climate and land cover change on stream discharge in the Ozark highlands, USA". Environmental Modelling and Assessment 10:9-19.

Humes, K. S., Kustas, W. P., Moran, M. S., Nichols, W. D and Weltz, M. A. (1994). "Variability of emissivity and surface temperature over a sparsely vegetated surface". Water resources research 30(5): 1299-1310.

Idowu, I. A and Muazu, K. M. (2010): "Mapping land use/land covers and change detection in Kafur Local Government, Katsina (1995-2008) Using Remote Sensing and GIS: Contemporary Issues in infrastructural development and management in Nigeria". Edited by A. Ogidiolu. Published by Department of Geography and Planning, Kogi State University Anyigba.

Isichei, A. O and Sandford, W. W. (1976). "The effects of waste gas flares on the surrounding vegetation of South-Eastern Nigeria". Applied Ecology 13: 177-187.

Jimenez-Munoz, J. C., Sobrino, J. A., Gillespie, A., Sabol, D and Gustafson, W. T. (2006). "Improved land surface emissivities over agricultural areas using ASTER NDVI". Remote Sensing of Environment 103: 474-487.

Jin, M., Dickinson, R. E and Vogelmann, A. M. (1997). "A comparison of CCM2/ BATS skin temperature and surface-air temperature with satellite and surface observations". Climate 10: 1505-1524.

ISSN 2054-6351 (print), ISSN 2054-636X (online)

Jin, M and Liang, S. (2006). "An improved land surface emissivity parameter for land surface models using Global Remote Sensing Observations". Journal of Climate 19: 2867-2881.

Kaufman, Y. J., Karnieli, A and Tanre, D. (2000). "Detection of dust over deserts using satellite data in the solar wavelengths". IEEE Transactions on Geoscience and Remote Sensing 38: 525-531.

Kayet, N., Chakrabarty, A., Pathak, K., Sahoo, S., Mandal, S. P., Fatema, S., Tripathy, S., Garai, U and Das. A. A. (2018). "Spatiotemporal LULC change impacts on groundwater table in Jhargram, West Bengal, India". Sustainable Water Resources Management. doi.org/10.1007/s40899-018-0294-9;

Labed, J and Stoll, M. P. (1991). "Spatial variability of land surface emissivity in the thermal infrared band: Spectral signature and effective surface temperature". Remote Sensing of Environment 38: 1-7.

Lambin, E. F., Geist, H. J and Lepers, E. (2003). "Dynamics of land use and land cover change in tropical regions". Annual Review of Environment and Resources. 28: 205-241.

Li, Z. L and Becker, F. (1993). "Feasibility of land surface temperature and emissivity determination from AVHRR data". Remote Sensing of Environment 43: 65-85.

Liang, S., Fallah-Adl, H., Kalluri, S., JaJa, J., Kaufman, Y and Townshend, J. (1997). "Development of an operational atmospheric correction algorithm for TM imagery". Journal of Geophysical Research 102: 17173-17186.

Liang, S. (2001). "An optimization algorithm for separating land surface temperature and emissivity from multispectral thermal infrared imagery". IEEE Transaction on Geoscience and Remote Sensing 39: 264-274.

Liang, S., Ed. (2004). "Quantitative Remote Sensing of Land Surfaces", John Wiley and Sons

Maaharjan, A. (2018). "Land use/land cover of Katnmandu valley by using Remote Sensing and GIS". M.Sc. Dissertation submitted to Central Department of Environmental Science, Institute of Science and Technology, Tribhuvan University, Kirtipur, Kathmandu, Nepal.

Mallick, J., Singh, C. K., Shashtri, S., Rahman, A and Mukherjee, S. (2012). "Land surface emissivity retrieval based on moisture index from Landsat TM satellite data over heterogeneous surfaces of Delhi city". International Journal of Applied Earth Observation and Geoinformation 19: 348-358.

Masuda, K., Takashima, T and Takayama, Y. (1988). "Emissivity of pure and sea waters for the model sea surface in the Infrared Window Regions". Remote Sensing of Environment 24:313-329.

Mather, P. M. (2004). "Computer processing of remotely sensed images: An Introduction", 3rd Edition. West Sussex, England, John Willey and Sons.

Mmom, P. C and Fred-Nwagwu, F. W. (2013). "Analysis of land use and land cover change around the city of Port Harcourt, Nigeria". Global Advanced Research Journal of Geography and Regional Planning (ISSN: 2315-5018) 2(5): 76-86.

Morakinyo, B. O. (2015). "Flaring and pollution detection in the Niger Delta using Remote Sensing". Unpublished Ph.D Thesis, School of Marine Science and Engineering, University of Plymouth, Plymouth, UK.

NASA. (2002). National Aeronautics and Space Administration. "Landsat 7 ETM+ Science Data Users Handbook". [Online]. Available:

ISSN 2054-6351 (print), ISSN 2054-636X (online)

http://www.landsathandbook.gsfc.nasa.gov/data_prod/prog_sect11_3.html [Accessed 23rd January 2017].

Niehoff, D., Fritsch, U and Bronstert, A. (2002). "Land-use impacts on storm-runoff generation: Scenarios of land-use change and simulation of hydrological response in a meso-scale catchment in SW-Germany". Journal of Hydrology 267: 80-93.

Nnaji, A. O., Njoku, E. R and Chibuike, P. C. (2016). **"**Spatio temporal analysis of land use/land cover changes in Owerri municipal and its environs, Imo State, Nigeria". Sky Journal of Soil Science and Environmental Management, 5(2): 33-43.

Odukoya, O. A. (2006). "Oil and sustainable development in Nigeria: A case study of the Niger Delta". Human Ecology 20(4): 249-258.

Okde, A. S (2006). "Land cover change along the Lagos Coastal area". Unpublished PhD Dissertation, Department of Geography, University of Ibadan, Nigeria.

Olowolafe, E. A., Bamike, T. J and Ishaya, S. (2010). "Remote sensing and GIS application in assessing changes in land use in Barkin-Ladi of Plateau State, Nigeria: Contemporary issues in infrastructural development and management in Nigeria". Edited by A. Ogidiolu. Published by Department of Geography and Planning, Kogi State University Anyigba.

Onosode, G. O. (2003). "Environmental issues and challenges of the Niger Delta (Perspectives from the Niger Delta Environmental Survey Process)". Lagos, Lilybank Property and Trust Limited.

Ouedraogo, I., Tigabu, M., Savadogo, P., Compaore, H., Ode´N, P. C and Ouadba, J. M. (2010). "Land covers change and its relation with population dynamics in Burkina Faso, West Africa". Wiley Inter Science, Land Degradation & Development. 21:453-462.

Pareta, K. (2014). **"**Land use and land cover changes detection using multi-temporal satellite data". International Journal of Management and Social Sciences Research 3(7): 10-17.

Patrono, A. (1996). "Synergism of remotely sensed data for land cover mapping in heterogeneous alpine areas: an example combining accuracy and resolution". ITC Journal 2: 101-109.

Peng, D. Q., Chen, Y. H., Li, J., Zhou, J and Ma, W. (2008). "Research on urban surface emissivity based on unmixing pixel". The International Archives of the Photogrammetry, Remote Sensing and Spatial Information Sciences, vol. XXXVII, Beijing, Part B6b.

PTT. (2008). "Flaring and venting philosophy". [Online]. Available: http:// www. Scribd.com/doc/108536828/Flaring-and-Venting-Philosophy [Accessed 12th February 2017].

Pu, R., Gong, P., Michishita, R and Sasagawa, T. (2006). "Assessment of multi-resolution and multi-sensor data for urban surface temperature retrieval". Remote Sensing of Environment 104: 211-225.

Qin, Q., Zhang, N., Nan, P and Chai, L. (2011). "Geothermal area detection using Landsat ETM+ thermal infrared data and its mechanistic analysis: A case study in Tengchong, China". International Journal of Applied Earth Observation and GeoInformation 13: 552-559.

Rahman, A., Kumar, S., Fazal., S and Siddiqui, M. A. (2012). "Assessment of land use/land cover change in the North-West District of Delhi using Remote Sensing and GIS Techniques". Indian Society of Remote Sensing.

ISSN 2054-6351 (print), ISSN 2054-636X (online)

Reid, R. S, et al. (2005). "Global changes in land cover". Update Newsletter of the International Human Dimensions Programme on Global Environmental Change 03, pp. 45.

Ringrose, S., Vanderpost, C and Maheson, W. (1997). **"**Use of image processing and GIS technique to determine the extent and possible causes of land management/fence line induced degradation problems in the Okavango area, Northern Botswana". International Journal of Remote Sensing 8(11): 2337-2364.

Roberts, D. A., Bastita, G. T., Pereria, S. L. G., Waller, E. K and Nelson, B. W. (1998). "Change Identification Using Multitemporal Spectral Mixture Analysis-Applications in Eastern Amazonia" in Lunetta, R. S, Elvidge, C. D (eds) Remote Sensing and 21 Change Detection Environmental Monitoring Methods and applications. Sleeping Bear Press Inc. Michigan.

Sáez, A. (2010). "Industrial application of natural gas". [Online]. Available: http://www.intechopen.com/books/natural-gas/industrial-applications-ofnatural-gas [Accessed 1st March 2017].

Santer, R., Carrere, V., Dubuisson, P and Roger, J. C. (1999). "Atmospheric correction over land for MERIS". International Journal of Remote Sensing 20: 1819-1840.

Şatır, O and Berberoğlu, S. (2012). "Land use/cover classification techniques using optical remotely sensed data in landscape planning". Landscape Planning, Dr. Murat Ozyavuz (Ed.), ISBN: 978-953-51-0654-8, InTech. [Online]. Available: http://www.intechopen.com/books/landscapeplanning/land-use-cover-classificationtechniques-using-optical-remotelysensed-data-in-landscape-plannin [Accessed 15th May 2018].

Schulze, R. E. (2000). "Modelling hydrological responses to land use and climatic change: The Southern African perspective". Journal of the Human Environment. 29:12-22.

Shravya, S and Sridhar, P. (2017). "Land use and land cover change detection for Delhi Region through Remote Sensing Approach". International Journal for Scientific Research & Development 4(11).

Shore, D. (1996). "Making the flare safe". Journal of Loss Prevention in the Process Indusrties 9(6).

Snyder, W. C., Wan, Z., Zhang, Y and Feng, Y. Z. (1998). "Classification-based emissivity for land surface temperature measurement from space". International Journal of Remote Sensing 19: 2753-2774.

Stathopoulou, M and Cartalis, C. (2007). "Daytime urban heat island from Landsat ETM+ and corine land cover data: An application to major cities in Greece". Solar Energy 81: 358-368.

Tan, S and Zhang, J. (2008). "An empirical study of sentiment analysis for Chinese documents". Expert Systems Applications 34(4): 2622-2629.

Teillet, P. M and Fedosejevs, G. (1995). "On the dark target approach to atmospheric correction of remotely sensed data". Canada Journal of Remote Sensing 21: 374-387.

Tokula, E. A and Ejaro, S. P. (2012). "Dynamics of land use/land cover changes and its implication on food security in Anyigba, North Central, Nigeria". Confluence Journal of Environmental Studies (CJES), Kogi State University, Anyigba, Nigeria.

Tomar, S., Saha, A., Kumari, M and Somvanshi, S. (2017). "Land use and land cover change monitoring of Surajpur Wetland, Uttar Pradesh: using GIS and Remote Sensing Techniques". 17th Esri India User Conference.

ISSN 2054-6351 (print), ISSN 2054-636X (online)

Tzotsos, A and Argialas, D. (2008). "Support vector machine classification for object-based image analysis". In: Blaschke T, Lang S, Hay GJ (eds) Object-based image analysis. Springer, Berlin, Heidelberg, pp 663-677.

UNEP. (2011). United Nations Environment Programme. "Environmental Assessment of Ogoniland". Nairobi, Kenya: pp 1-248. [Online]. Available: http://www.unep.org/disasterandconflicts/CountryOperations/Nigeria/EnvironmentalAssessmentofOgonilandreport/tabid/54419/Default.aspx [Accessed 5th July 2017].

van de Griend, A. A., Owe, M., Groen, M and Stoll, M. P. (1991). "Measurement and spatial variation of thermal infrared surface emissivity in a savanna environment". Water Resources Research 27: 371-379.

van de Griend, A. A and Owe, M. (1993). "On the relationship between thermal emissivity and the normalized difference vegetation index for natural surfaces". International Journal of Remote Sensing 14: 1119-1131.

Verburg, P. H., Veldkamp, W. S. A., Espaldon, R. L. V and Mastura, S. S. A. (2002). "Modeling the spatial dynamics of regional land use: the CLUE-S Model". Environment Management 30(3): 301-405, Springer-Verlag, New York Inc.

Wan, Z and Dozier, J. (1996). "A generalized split-window algorithm for retrieving land surface temperature measurement from space". IEEE Transactions on Geoscience and Remote Sensing 34: 892-905.

Wan, Z. and Li, Z. (1997). "A physics-based algorithm for retrieving land-surface emissivity and temperature from EOS/MODIS data". IEEE Transaction on Geoscience and Remote Sensing 35 (4): 980-996.

Xu, W., Wooster, M. J. and Grimmond, C. S. B. (2008). "Modelling of urban sensible heat flux at multiple scales: a demonstration using airborne hyperspectral imagery of Shanghai and a temperature-emissivity separation approach". Remote Sensing of Environment 112: 3493-3510.

Yeboah, F., Awotwi, A and Korkuo, E. K. (2017). "Assessing the land use and land cover changes due to urban growth in Accra, Ghana". Journal of Basic and Applied Research International 22(2): 43-50.

Yue Chang, Y., Hou, K., Li., X., Zhang, Y and Chen, P. (2018). "Review of land use and land cover change research progress". IOP Conference Series: Earth and Environmental Science 113 012087 doi :10.1088/1755-1315/113/1/012087).

Yuechen Liu, Y., Pei, Z., Wu, Q., Guo, L., Zhao, H and Chen, X. (2012). **"**Land use/land cover classification based on Multi-resolution Remote Sensing Data. International Federation for Information Processing AICT 369: 340-350.

Zhu, T. G. L. D. (2006). "Thermal Remote Sensing". Publishing House of Electronics Industry, Beijing, China.

ISSN 2054-6351 (print), ISSN 2054-636X (online)